Shape of the liquid-vapor coexistence curve for temperature and density dependent effective interactions

S. Amokrane* and M. Bouaskarne
Groupe de Physique des Milieux Denses, Faculté des Sciences et de Technologie, Université Paris XII, 61 Avenue du Général de Gaulle, 94010 Créteil Cedex, France

(Received 29 November 2001; published 24 April 2002)

The asymmetry of the coexistence curve that is observed in several micellar systems is discussed in relation with the dependence of the effective interaction on temperature and density. Standard results for the diameter of the coexistence curve in the van der Waals theory are generalized so as to deal with this combined dependence. The qualitative trends so deduced are assessed by comparison with coexistence curves of Yukawa fluids computed with integral equation theories. The role of the variables used to plot the coexistence curve and the nonlinear behavior of its diameter beyond the critical region are discussed in relation with the decrease of the interaction strength with density. The possibility of using the asymmetry of the coexistence curve as an indicator of the state dependence of the effective interaction is finally discussed.

DOI: 10.1103/PhysRevE.65.051501 PACS number(s): 64.70.Fx, 64.60.−i, 82.70.−y

I. INTRODUCTION

Effective interactions that depend on the thermodynamic variables are often considered in the physics of liquids. This dependence follows either from theoretical considerations or is introduced as a necessity for interpreting experimental observations. An example is the case of asymmetric solute-solvent mixtures described at the McMillan-Mayer level [1]. A prototype of this situation is the Deryaguin-Landau-Verwey-Overbeek (DLVO) potential in charge stabilized colloidal dispersions in which temperature enters the inverse Debye length [2]. State dependent interactions are also introduced for interpreting scattering measurements in nonionic dispersions such as colloidal silica particles (see, for example, Refs. [3–5]) or reverse micelles in organic solvents (see, for example, Refs. [6–9]). For these systems, the effective interaction fitted to experiment is found to depend on density and/or temperature or even on the pressure (see, for example, Refs. [10]). In a different context, one may view the effective interaction between ions in liquid metals as belonging to this class since it depends on the electronic density. The thermodynamic properties of the system—in particular the liquid vapor coexistence curve, or its equivalent in the effective fluid representation—can be affected by this dependence up to the qualitative level. To take the example of temperature, profound changes with respect to simple fluids are evidenced by the lower consolute points shown by several micellar systems [8]. The strong asymmetry of the coexistence curve and the unusually low critical volume fraction also favor an effective interaction that depends of the volume fraction of the dispersed phase. The asymmetry of the liquid vapor coexistence curve of liquid metals (see, for example, Ref. [11]) might also indicate such an effect.

Of course, these well-known features have already been discussed in the literature. The role of many body forces [12,13] or more generally that of state dependent intermolecular potentials [14] have in particular been underlined in some theoretical studies. The methods used in these studies—such as the effective Landau-Ginsburg-Wilson (LGW) Hamiltonian—being specially appropriate to the investigation of the critical behavior [15], the emphasis was naturally put on the critical region. A good understanding of some universal features, especially the singularity of the diameter of the coexistence curve close to the critical point, has been gained in this manner. For a more quantitative study of specific systems, a more standard approach can, however, be preferable. This is the case in the present work that was actually motivated by some experimental studies of micellar systems. The latter often show transitions similar to the liquid-vapor one in simple fluids [8]. These transitions were discussed with the help of theoretical coexistence curves relative to state independent interactions whereas structural data suggest that one is actually dealing with density dependent ones. A clarification of this point seems thus necessary, especially when the dependence on density combines with a simultaneous dependence on temperature. The latter has indeed been considered—separately—more often (see, for example, Ref. [16] for a recent study of a temperature dependent double Yukawa potential). The study of Reatto and Tau [13] in particular dealt with the effect of temperature or density in micellar system but on rather unspecific grounds. A more quantitative study seems thus useful. To this end, theoretical methods that enable a quantitative determination of the coexistence curve, including the precise location of the critical point, are required. The LGW Hamiltonian being not particularly designed for this purpose, we considered the integral equations of the theory of liquids [17] in which the microscopic parameters of the system can be incorporated more explicitly. Phase diagrams for a variety of state independent interactions (see, for example, Ref. [18] and references therein) have been obtained in this way but the situation is clearly different for state dependent ones.

The main purpose of this work is hence to discuss the effect on the coexistence curve of an effective interaction of the form $\epsilon(\rho,T)\ f(r)$. This specific form followed from our

*Author to whom correspondence should be addressed. Email address: amokrane@univ-paris12.fr

previous study [19] of the hard core Yukawa fluid as a model of the effective interaction in water in oil microemulsions. From this example, we will discuss some aspects of the state dependence that might be relevant in more general situations. In order to gain a qualitative understanding of the role of this T-ρ dependence, we first start with the van der Waals (vdW) theory. Standard results from the literature [15,20,21], including the effect of the ρ dependence of the slope of the diameter of the coexistence curve (see Ref. [12]) are generalized to an interaction strength that depends also on T. Next, a more quantitative discussion is performed with the help of integral equations methods, especially with that proposed by Duh and Mier-Y-Teran for Yukawa fluids [22]. As shown in our previous work [19], it can readily be adapted to study a temperature and density dependent effective interaction as that used to analyze micellar systems in organic solvents [8]. This method is both accurate and simple enough to permit a discussion well beyond the mean field van der Waals theory. It is indeed much simpler than the more accurate modified hypernetted chain (MHNC) integral equation [23], in its reference version (RHNC) [24] that we used for comparison (the difficulty in using the MHNC was, for instance, pointed out by Reatto and Tau [13] in their study of the coexistence curve of micellar systems). To this end, this paper is organized as follows. In Sec. II we present the expression of the diameter of the vdW coexistence curve for T-ρ dependent potentials together with a brief summary of the method used to compute the coexistence curve for the T-ρ Yukawa fluid. In Sec. III, we show and discuss some representative results and the paper ends with a conclusion.

II. COEXISTENCE CURVE FOR A TEMPERATURE AND DENSITY DEPENDENT INTERACTION STRENGTH

A. van der Waals theory

To begin with, we recall here the results relative to the coexistence curve and its diameter in the vdW theory. The starting point is the equation of state,

$$P=\frac{\rho k_B T}{(1-\rho b)}-a\rho^2, \tag{1}$$

where $a=\frac{1}{2}\int d\mathbf{r}\phi_{attr}(\mathbf{r})$ and $b=(2\pi/3)\sigma^3$ are the usual vdW parameters, $\phi_{attr}(r)$ being the attractive part of the interaction potential, beyond the hard-core diameter σ. The densities ρ_g and ρ_l of the gas and the liquid at equilibrium at a temperature T are obtained from the equality of the pressure and chemical potential of the coexisting phases:

$$P(\rho_l)=P(\rho_g);\quad \mu(\rho_l)=\mu(\rho_g). \tag{2}$$

The classical behavior of the diameter of the coexistence curve $\rho_d=(\rho_g+\rho_l)/2$ is obtained by assuming that the free energy F is an analytical function of T and ρ near and at the critical point [21] (this assumption must of course be reconsidered in a more rigorous treatment of the critical region [21]. See also the model of Widom and Rowlinson [25] for this point and for a general discussion of the diameter). $\rho_d(T)$ near T_c can then be obtained from a double Taylor expansion of F with respect to $r=(\rho-\rho_c)/\rho_c$ and $\tau=(T-T_c)/T_c$ (the subscript c stands for quantities computed at the critical point). Following Levelt-Sengers's derivation [20], the first term beyond $\rho_d=\rho_c$ is obtained by using in Eq. (2) the expansion of the pressure as

$$\frac{P}{P_c}=\sum_{m,n}\frac{1}{m!}\frac{1}{n!}p_{mn}r^m\tau^n, \tag{3}$$

where

$$p_{mn}=\frac{1}{P_c}\rho_c^m T_c^n\frac{\partial^{m+n}}{\partial\rho^m\partial T^n}P\Big|_{\rho_c,T_c},$$

and a similar expansion of the chemical potential μ. By assuming that the gas and liquid densities at coexistence have the expansion $r_l=a_1|\tau|^m+a_2|\tau|^{2m}+\cdots$ and $r_g=b_1|\tau|^m+b_2|\tau|^{2m}+\cdots$ one obtains from the lowest-order terms of Eq. (2): $m=\frac{1}{2}$, $a_1=-b_1$, and $a_2=b_2$. The reduced diameter $d=\rho_d/\rho_c$ is thus found to be linear in temperature: $d=1+a_2|\tau|$, with a slope given by [20]

$$a_2=\frac{p_{21}}{p_{30}}-\frac{3}{5}\frac{p_{11}p_{40}}{p_{30}^2}+\frac{4}{5}\frac{p_{11}}{p_{30}}. \tag{4}$$

From Eq. (1) one finds [20] $a_2=\frac{2}{5}$. For the forthcoming discussion, the main point is that Eq. (4) follows from the terms of order $\tau^{5/2}$ in the expansion of Eqs. (2).

We consider now the modifications due to the state dependence of the interaction, starting first with the dependence on ρ. In their study of the influence of three-body interactions on the vdW coexistence curve, Pestak *et al.* [12] supplemented the vdW free energy by a term quadratic in density: $F/N=F^{vdW}/N+q\rho^2$. The pressure $P=\rho^2[\partial(F/N)/\partial\rho]$ then reads

$$P=\frac{\rho k_B T}{(1-\rho b)}-a\rho^2-2q\rho^3, \tag{5}$$

where q is the equivalent of a for the three-body potential. The influence of the additional term proportional to q can be seen by expanding all quantities with respect to the small parameter $x=q/ab$, in which case the influence of q can be discussed without having to solve Eq. (2). This amounts to assuming that the strength of the attractive part of the three-body term is small with respect to the two-body potential term $\phi_{attr}(r)$. The critical density and critical temperature are obtained from the condition

$$\left.\frac{\partial P}{\partial\rho}\right|_{T_c}=\left.\frac{\partial^2 P}{\partial\rho^2}\right|_{T_c}=0 \quad \text{as} \quad \rho_c=\frac{1}{3b}\left(1+\frac{2}{3}x\right)$$

and

$$T_c=\frac{8a}{27b}(1+x),$$

where the prefactors are the pure vdW results ($q=0$). A similar expansion of Eq. (4) gives the new slope of the diameter as [12] $a_2=\frac{2}{5}+(22/15)x$.

More generally, one can view these modified vdW results as pertaining to an attractive interaction of the form $\phi_{attr}(r)=\epsilon(\rho)\ f(r)$ with $\epsilon(\rho)=\epsilon_o+\epsilon_1\rho$. If the linear term is small with respect to the constant term over a range of densities of the order of $\rho_{c,0}=1/3b$, that is, $\epsilon_1\rho_c\approx\epsilon_1\rho_{c,0}\ll\epsilon_o$, the smallness criterion remains $x\ll 1$. These results then show that within the vdW theory, a decrease of the strength of the attractive part of the effective potential energy lowers the critical temperature and critical density and increases the asymmetry of the coexistence curve. These features common to several micellar systems have also been discussed by Reatto and Tau [13] from a lattice gas model within the LGW Hamiltonian approach.

We now consider the generalization of these results for a strength of $\phi_{attr}(r)$ that depends also on temperature. To this end, the following model was considered:

$$\epsilon(\rho,T)=k_BT(\epsilon_o+\gamma T+\epsilon_1\rho). \tag{6}$$

This model is a simplified version of the strength $\epsilon(\rho,T)$ of the Yukawa interaction [see Eq. (20) below] that we used in our previous work [19] to analyze structural data and the coexistence curve of water in oil reverse micelles:

$$\phi(r)=\begin{cases}\infty, & r<\sigma\\ -\epsilon(\rho,T)\exp\{-\lambda(r/\sigma-1)\}/r, & r\geqslant\sigma,\end{cases} \tag{7}$$

where λ is the inverse range (in reduced units) of the attractive tail [because of the particular dependence on T involved in the definition (6), a temperature independent $\phi(r)$ is not recovered by setting $\gamma=0$]. For this model, the vdW equation of state reads

$$P=\frac{\rho k_BT}{(1-\rho b)}-a_0(T)\rho^2-a_1(T)\rho^3, \tag{8}$$

where $a_0(T)=ck_BT(\epsilon_o+\gamma T)$ and $a_1(T)=2ck_BT\epsilon_1$ with a mean field constant

$$c=2\pi\left(\frac{1}{\lambda}+\frac{1}{\lambda^2}\right).$$

It is useful to consider first the pure T dependence, obtained by setting $\epsilon_1=0$ in Eq. (6). The usual vdW form is thus recovered but with a temperature dependent attractive term $a_0(T)$. The only independent variable in an isothermal construction being $\epsilon^*=\epsilon(T)/k_BT$, the results at the critical point have the usual form $\rho_{c,0}=1/3b$, $k_BT_{c,0}=8a_0(T_{c,0})/27b$ and $P_{c,0}=a_0(T_{c,0})/27b^2$ independently of the specific form of $\epsilon(T)$ (the index 0 stands for $\epsilon_1=0$). The law of corresponding states thus holds, as long as $\epsilon(\rho,T)$ is independent of ρ. In these expressions, the critical temperature is given by

$$T_{c,0}=\frac{1}{\gamma}\left(\frac{27}{8}\frac{b}{c}-\epsilon_o\right). \tag{9}$$

The reduced interaction strength at the critical temperature $\epsilon(T_{c,0})/k_BT_{c,0}=\epsilon_o+\gamma T_{c,0}$ is also equal to that for a temperature independent interaction,

$$\frac{\epsilon}{k_BT_c}=\frac{27}{8}\frac{b}{c}$$

as will be detailed in the next section. The only nontrivial point concerns the slope of the diameter. Indeed, Eq. (4), involves derivatives with respect to the actual temperature and is *a priori* dependent on the linearity of Eq. (1) with respect to T. We examine this point below, together with the dependence on ρ.

As shown in Sec. 1 of the Appendix, with $\epsilon_1\neq 0$, one obtains at lowest order the critical density and critical temperature as

$$\rho_c=\frac{1}{3b}\left(1+\frac{2}{3}\frac{\epsilon_1}{(\epsilon_o+\gamma T_{c,0})b}\right), \tag{10}$$

$$T_c=T_{c,0}-\frac{\epsilon_1}{\gamma b}, \tag{11}$$

with $T_{c,0}$ given by Eq. (9). The influence of the density dependence is obvious from Eqs. (10) and (11), the main point being the lowering of ρ_c when $\epsilon_1<0$, as with T independent interactions.

A discussion of the diameter prior to the Maxwell construction requires the new expression of a_2. It is shown in Sec. 2 of the Appendix that (4) giving a_2 in terms of the coefficients p_{ij} keeps the same form, the latter being of course modified. By using Eqs. (10) and (11) in Eq. (4), one can obtain a small x expansion of a_2 but the resulting expression is too cumbersome to be shown here. A simple result follows when $\epsilon_1=0$ (pure T dependence);

$$a_2=\frac{2}{5}\left(1-\frac{8c}{27b}\frac{\epsilon_o+\gamma T_{c,0}}{T_{c,0}}\right). \tag{12}$$

Besides these analytical expressions, one can construct the full coexistence curve and its diameter by solving Eq. (2). Rather than proceeding by graphical determination of the common tangent on the free-energy isotherms, one can rearrange Eq. (2) in the form (see also Ref. [26])

$$P(\rho_l)\left(\frac{1}{\rho_g}-\frac{1}{\rho_l}\right)=\int_{\rho_g}^{\rho_l}\frac{d\rho}{\rho^2}(P-\rho k_BT)-k_BT\ln\left(\frac{\rho_l}{\rho g}\right) \tag{13}$$

that is more suitable for numerical calculations.

The predictions from the mean field vdW theory being limited to the qualitative level, two integral equations methods that we used for a more quantitative study are briefly described below.

B. Coexistence curve from the RHNC and MSA integral equations

The first one is the well-known RHNC integral equation [24] that supplements the Ornstein-Zernike equation [17] for the total and direct correlation functions $h(r)=g(r)-1$ and $c(r)$,

$$h(r)-c(r)=\rho\int d\mathbf{r}'h(r')c(|\mathbf{r}-\mathbf{r}'|) \tag{14}$$

by the closure

$$g(r)=\exp[-\phi(r)/k_BT+h(r)-c(r)-b_0(r)], \tag{15}$$

where $b_0(r)$ is the bridge function of a reference system, here a system of hard spheres, whose diameter is determined by the optimization condition [24]

$$\int d\mathbf{r}[g(r)-g_0(r)]\frac{\partial b_0(r)}{\partial\sigma}=0. \tag{16}$$

The RHNC has been applied to a variety of state independent interactions and has been shown to be very accurate when compared with simulation (see, for example, Refs. [27,18] and references therein). In this work, we used the parametrization of $b_0(r)$ of Malijevsky and Labik [28] and used the algorithm of Labik *et al.* [29] for solving Eqs. (14)–(16). One major difficulty with the RHNC and related methods is the presence of a domain near the critical point where numerical convergence is impossible (see, however, Ref. [30] for a possible way to circumvent this problem and Ref. [31] for improving convergence at high density). Since the interaction potential $\phi(r)$ appears explicitly in the closure (15), this method can be used as it stands to compute $g(r)$ for state dependent ones. This holds also for the RHNC free energy that is obtained from the energy route [see Eqs. (8)–(10) in our previous work [19]]. The construction of the RHNC coexistence curve being rather lengthy, it has been used here only for checking the results of a much simpler method that we detail now.

The second method is specially designed for the hard-core Yukawa interaction (7). It is based on the inverse temperature expansion of the free energy (ITEF) in the mean spherical approximation (MSA), that is with the closure $c(r>\sigma)=-\phi(r)/k_BT$. The original expansion [32] of the excess free energy $\Delta f=(F-F_0)/Nk_BT$ with respect to that of hard spheres, as an infinite series of the reduced strength $\epsilon^*=\epsilon/k_BT$, is

$$\Delta f=-\frac{1}{2}\sum_1^\infty\frac{V_n}{n}(\epsilon^*)^n. \tag{17}$$

This was deduced from the analytical solution [33] and was later summed by Duh and Mier-Y-Teran [22] who extended the expression of the coefficients V_n. The resulting closed form of Δf involves explicit functions of the packing fraction $\eta=\pi/6\rho\sigma^3$ (see Ref. [22] for the expression of the various terms). Our previous work [19] has shown that this form of Δf can be used even with an effective interaction strength ϵ that depends on ρ and T. However, the pressure involves additional terms related to $\partial\epsilon^*(\rho,T)/\partial\rho$. From the explicit expression of P given in Ref. [19], the coexistence curve is readily determined by numerical solution of Eq. (13). These results are presented and discussed below.

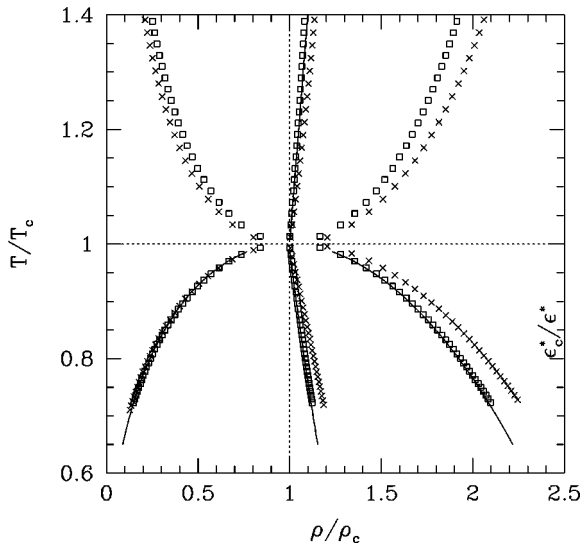

FIG. 1. Reduced temperature and reduced inverse interaction strength vs reduced density along the coexistence curve. Data above the line $y=1$: density independent interaction ($\epsilon_1=0$, squares) and density dependent one ($\epsilon_1=-0.157$, crosses). The line is the linear diameter for $\epsilon_1=0$ with slope given by Eq. (12). Data below the line $y=1$: full curves represent coexistence curve and its diameter for temperature independent interaction (the left and right y scales are equal). Symbols: inverse reduced interaction strength along the coexistence curve and its diameter; squares ($\epsilon_1=0$, left and right scales are equal). Crosses ($\epsilon_1=-0.157$, right scale only).

III. RESULTS AND DISCUSSION

A. van der Waals coexistence curve for T-ρ dependent interaction strength

Besides the analytical considerations of the previous section, the point we wish to discuss here is the relative influence of the variation of $\epsilon(\rho,T)$ with T and that with ρ on the asymmetry of the vdW coexistence curve. Figure 1 shows typical results obtained from a numerical solution of Eq. (13) with the following values of the parameters in $\epsilon(\rho,T)$ of Eq. (6): $(\epsilon_0,\gamma,\epsilon_1)=(0.5,0.2,0)$ and $(0.5,0.2,-157)$ [$\epsilon_1=-0.157$ is actually $0.3\pi/6$]. These values were chosen so as to keep up with the low x expansion discussed above. The point to be noted is the role of the energy scale used to plot these curves. When the reduced strength ϵ_c^*/ϵ^* is used for the y axis (part of the plot below the line $y=1$), the coexistence curve for the model (6) with $\epsilon_1=0$ is the same as the pure vdW one [with a pure $\epsilon(T)$ variation, the law of corresponding states holds as discussed in Sec. II A]. Note that ϵ_c^*/ϵ^* equals $(\epsilon_o+\gamma T_{c,0})/(\epsilon_o+\gamma T)$ and T/T_c, respectively, where T is the actual temperature in kelvin. On the contrary, when T/T_c is used, the pure vdW curve remains the same but different curves lying above the line $y=1$ are obtained for

each value of the ratio γ/ϵ_o in the law $\epsilon(T)$. Incidentally, the variation with T embodied in Eq. (6) restores symmetry with respect to the pure vdW curve. Besides the fact that the usual behavior is recovered when the ''natural'' variable ϵ_c^*/ϵ^* is used, the MSA results presented below show that this is not the generic behavior when $\epsilon(T)$ increases with T. The main point here is that the coexistence curves have different aspects in the representations $T/T_c-\rho/\rho_c$ and $\epsilon_c^*/\epsilon^*-\rho/\rho_c$, but both have the same status. In particular, two conjugate points correspond to a constant T or ϵ^*.

The situation is different when $\epsilon_1\neq 0$, since each value of ϵ_1/ϵ_o gives a different curve even in the ϵ_c^*/ϵ^* representation. This last situation involves indeed two independent energy variables [see Eqs. (6)–(8)]. In addition, $\rho_g(T)$ and $\rho_l(T)$ determined at fixed T do not correspond to the same value of ϵ_c^*/ϵ^* because of the density dependence of $\epsilon(\rho,T)$. The curve $\epsilon_c^*/\epsilon^*-\rho/\rho_c$ then loses the meaning of a coexistence curve since it does not correspond to the locus of conjugate points as defined in Ref. [25]. The tielines connecting such points are given by a linear equation $\epsilon(\rho)=c+d\rho$, with different values of c and d at each T [see Eq. (6)]. The vapor and the liquid branches, nevertheless, form a single continuous curve that actually corresponds to the variation of the reduced interaction strength $\epsilon_c^*/\epsilon^*(\rho)$ along the coexistence curve. One can also draw its variation $\epsilon_c^*/\epsilon^*(\rho_d)$ along the diameter $d\equiv 1/2\rho_c(\rho_g+\rho_l)=d[\epsilon(\rho_d(T),T)]$. Because of the weak dependence on ρ when $\epsilon_1=-0.157$, the tielines are almost parallel to the abscissa axis and the curve $\epsilon_c^*/\epsilon^*-\rho/\rho_c$ lies below the line $y=1$. Its maximum is almost indistinguishable from the location of the critical point. As shown below, the situation can be quite different when an accurate equation of state is used in conjunction with a different $\epsilon(\rho,T)$ law.

Finally, when $\epsilon_1=-0.157$, the strength $\epsilon(\rho,T)$ decreases with density at constant T, the coexistence curve (that is in the T/T_c scale) is more asymmetrical than when $\epsilon_1=0$. In view of this, the increased asymmetry associated with the decrease of $\epsilon(\rho,T)$ with ρ is not of a distinct nature than that discussed analytically in Sec. II A for the pure $\epsilon(\rho)$ form. The converse of this trend—the diameter becoming more vertical when $\epsilon(\rho,T)$ increases with ρ—is also natural.

The more interesting point is the long-known observation that the near linearity of the diameter extends well below the critical point (the so-called law of rectilinear diameters). We are not aware of a general explanation of this law, even in the context of the van der Waals equation. In this case, we found that some insight into this question might be gained by considering the situation $T\ll T_c$. By neglecting contributions due to ρ_g (see below), an explicit expression of the slope of $\rho_d(T)\approx\frac{1}{2}\rho_l(T)$ for $T\ll T_c$ can be obtained as follows: a useful starting point is Clapeyron's equation relating the temperature coefficient $(\partial P/\partial T)_\sigma$ along the coexistence curve to the latent heat of evaporation Δh (in Ref. [25], Widom and Rowlinson discussed also the behavior of ρ_g and ρ_l at low T in their model but from virial expansions). By using the relation $(\partial\Delta h/\partial T)_\sigma=\Delta c_p$ valid at low enough T [21], the equilibrium equation (13), and the relation specific to the vdW equation (1),

$$\left(\frac{\partial P}{\partial T}\right)_\rho=\frac{1}{T}(P+a\rho^2), \tag{18}$$

one gets (see the Appendix) the slope of ρ_l for $T\ll T_c$ as

$$\frac{d\rho_l}{dT}\simeq\frac{1}{a}(\Delta c_p-k_B)\simeq-(k_B/a)\left[1-\frac{2ak_BT}{\rho_l}\right]^{-1}. \tag{19}$$

The slope of the density in the vapor is more directly obtained as $d\rho_g/dT\simeq(a/kT^2)\rho_l\rho_g$. Equation (19) shows that ρ_l is not linear in T. However, it so happens that while the magnitude of the second term in the bracket is comparable to unity, it varies slowly with T. This is in accordance with the known fact that for several substances, Δc_p is almost constant at low enough T. A linear fit of the liquid branch in the range $0.4\leqslant T^*\leqslant 0.44$ $(T^*\equiv k_BT/\epsilon)$ gives, for instance, $d\rho_l/dT^*\simeq 0.304$ whereas Eq. (19) gives $0.3\leqslant d\rho_l/dT^*\leqslant 0.33$. Similarly, we find in the vapor branch $d\rho_g/dT^*\simeq 0.073$ whereas $(a/kT^2)\rho_l\rho_g$ varies between 0.06 and 0.07. This shows that for $T\ll T_c$, the slope of the diameter is mainly determined by $d\rho_l/dT$ which is roughly constant, because Δc_p behaves so. This result would hold for other equations of state showing a behavior similar to Eq. (18), that is, those keeping the quadratic and temperature independent mean field term, but with different hard sphere contributions. Even so, a more physical understanding of this near linearity of the diameter requires an explanation of the combination of the thermal and elastic coefficients that leads to this near constancy of Δc_p at low enough T.

B. Coexistence curve in the MSA

Since the vdW treatment is not expected to be quantitatively accurate, we examine now the results obtained from the MSA . We first considered the variation of $\epsilon(\rho,T)$ with ρ and T separately. Figure 2 shows the coexistence curve for $\epsilon(\rho)=\epsilon_o+\epsilon_1\rho$. For $\epsilon_1=0$, comparison with simulation data is possible. The agreement in absolute variables is satisfactory, except near the critical point [22]: the critical density is very good, $\rho_c^*\equiv\rho_c\sigma^3\simeq 0.316$ (to be compared with 0.313 by simulation) but the critical temperature is too high, $T_c^*\simeq 1.238$ while simulation [27] gives $T_c^*\simeq 1.177$. Beyond the critical point, the MSA is almost as accurate as the RHNC [27] [see also Fig. 3(a)]. The inaccuracy of the vdW critical values $\rho_c^*=1/2\pi\simeq 0.16$ and $T_c^*=\frac{8}{27}c\simeq 0.77$ is evident (these values correspond to a Yukawa inverse range $\lambda=1.8$). In reduced variables [Fig. 2(b)], the overestimation of the critical temperature by the MSA worsens the agreement with simulation but the diameter agrees with simulations better than the vdW one. The MSA diameter for $\lambda=1.8$ is in very good agreement with the experimental one [34], but this seems fortuitous. The slope of the diameter depends indeed slightly on λ, even in the units $T/T_c-\rho/\rho_c$ (by plotting the simulation data of Lomba and Almarza in reduced variables we also found that the diameter for $\lambda=3$ is clearly distinct from those for $\lambda=4$ and $\lambda=1.8$). It is also to be mentioned that according to Duh and Mier-y-Teran [22], their formula-

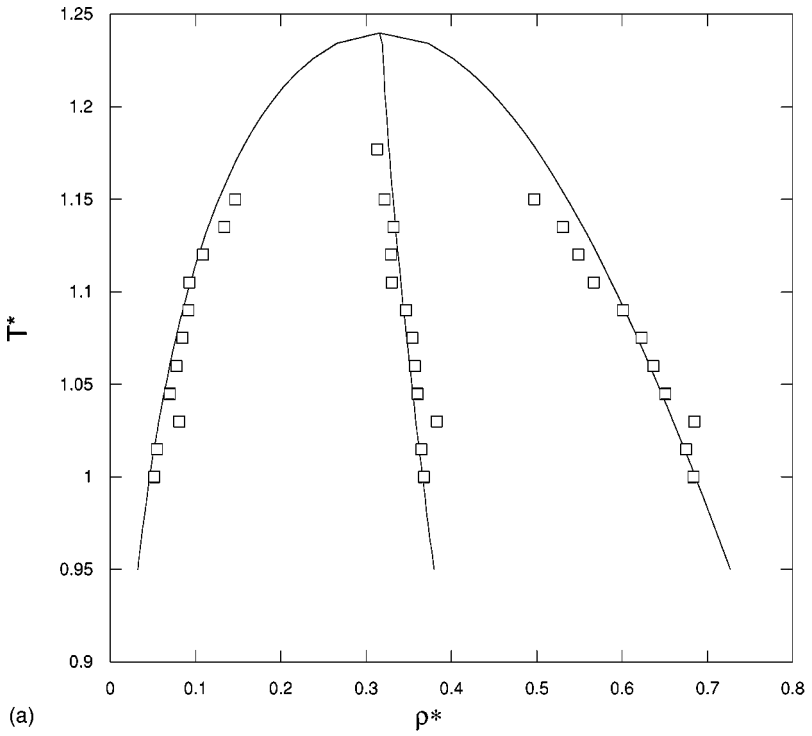

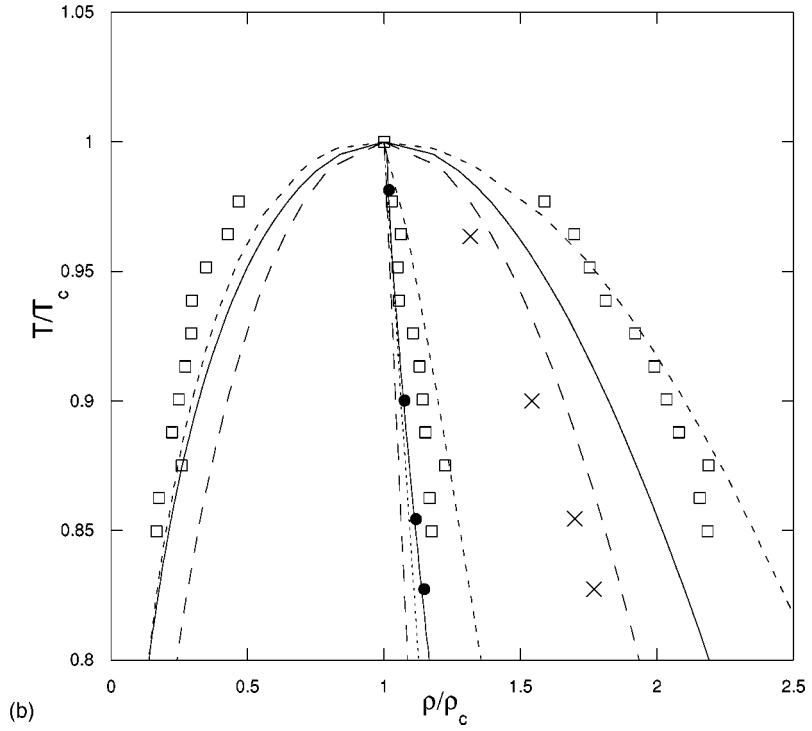

FIG. 2. (a) Coexistence curve in the temperature-density plane of the Yukawa potential with $\lambda = 1.8$. Full lines: coexistence curve and its diameter from the MSA [Eq. (17)]. Symbols: simulation data [27]. ϵ independent of T and ρ. (b) Coexistence curves and diameters in reduced variables. Full curves and squares: same as in Fig. 2(a). Short dashes: MSA for density dependent interaction ($\epsilon_1 = -0.157$). Black circles, experimental diameter [34]. Long dashes: van der Waals ($\epsilon_1 = 0$). Dots: van der Waals ($\epsilon_1 = -0.157$). Crosses: *diameter* for the sticky hard-sphere model [38].

tion of the MSA being based on the energy route, it is expected to yield classical mean-field critical exponents. Since in this work we were not particularly interested in the critical behavior, we did not consider this aspect further.

The main point now is that the MSA curve with $(\epsilon_o, \epsilon_1) = (0.5, -0.157)$ is clearly more asymmetrical than when ϵ_1 equals 0. The vdW predictions are correct at the qualitative level but the change predicted from $\epsilon_1 = 0$ to $\epsilon_1 = -0.157$ is not quantitatively significant. The last value corresponds to a decrease of $\epsilon(\rho)$ of about 25% from $\rho = 0$ to $\rho = 2.5\rho_c$. This moderate variation might thus correspond to real physical situations. In contrast with the vdW treatment, the MSA generates in these conditions a diameter that departs significantly from the experimental one for ordinary substances.

We now consider the additional variation with temperature on the example of the effective interaction in AOT (sodium bis di-ethylhexyl sulfosuccinate) reverse micelles. Figure 3 shows the coexistence curve obtained with $\epsilon(\rho, T)$

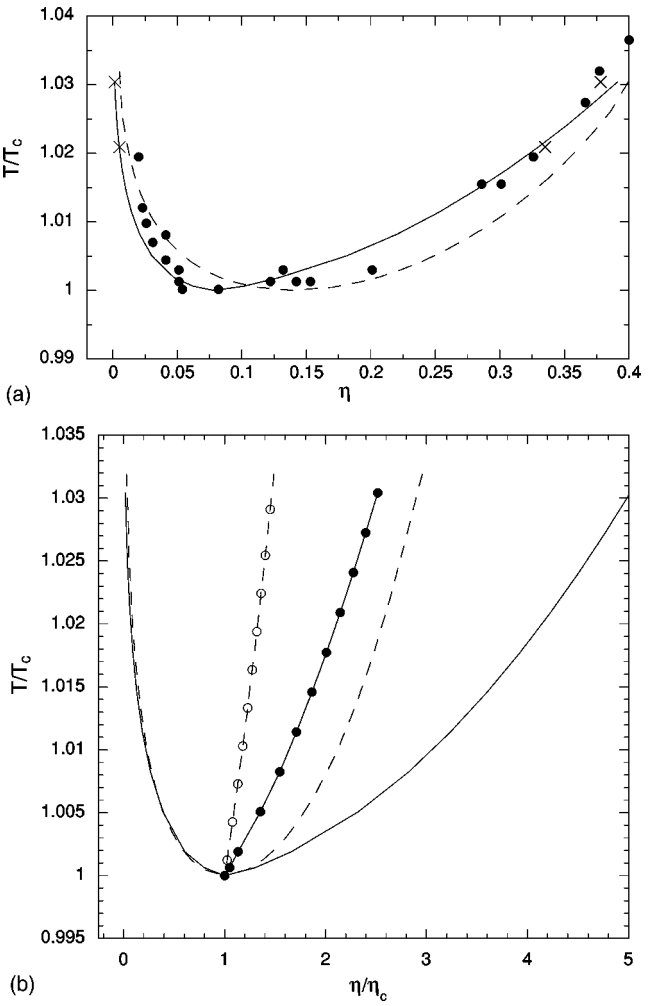

FIG. 3. (a) Coexistence curve for reverse micelles in the reduced temperature-packing fraction plane. Black circles: experimental data for the AOT water in decane system [8]. Full curve: MSA with $\epsilon^*(\eta,T)$ from Eq. (20) and $\lambda=1.2$ (see Ref. [19] for the values of the coefficients). Crosses: RHNC points, same law. Dashed curve: MSA for $\lambda=0.73$ and $\epsilon^*(\eta,T)$ independent of η [$b_0=0$ in Eq. (20)]. (b) Theoretical coexistence curves and diameter for reverse micelles in reduced variables. Curves: same as in Fig. 3(a). Symbols show the diameters: empty circles represent density independent $\epsilon(b_0=0)$, black circles represent density dependent $\epsilon(b_0\neq 0)$.

computed from

$$\epsilon^*(\eta,T)=a_0+a_1T+a_2T^2+b_0\exp(-b_1\eta) \qquad (20)$$

and an inverse range parameter $\lambda=1.2$. The other parameters were determined by fitting experimental data for the low-angle structure factor $S(q)$ by the equation

$$S^{-1}(q=0)=\frac{1}{k_BT}\left.\frac{\partial P}{\partial \rho}\right|_T.$$

The result obtained by ignoring the density dependence in Eq. (20) (parameters of Chen *et al.* [35] with $\lambda=0.73$) is given for comparison. In order to judge the accuracy of the

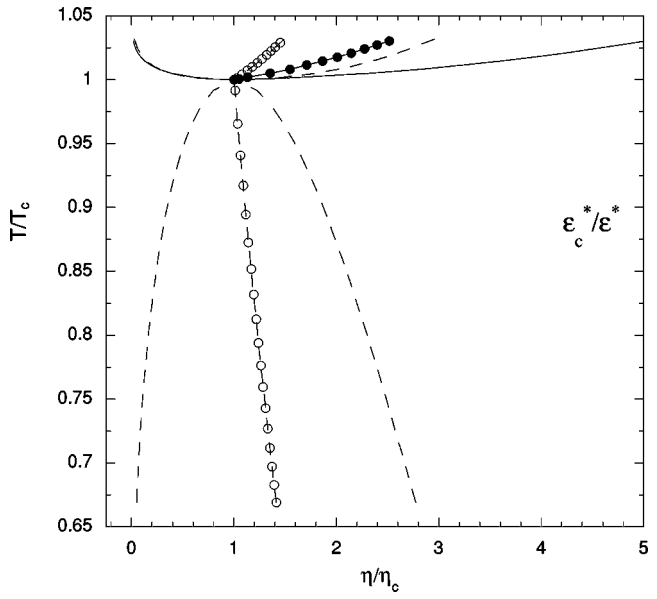

FIG. 4. Theoretical coexistence curves and diameter for reverse micelles in alternative scales. Curves above the line $y=1$: *same* as those in Fig. 3. The curve below the line $y=1$ is another representation of that for density independent $\epsilon(b_0=0,\lambda=0.73)$. With the right scale, it is the transform of the dashed curve above the line $y=1$. With the left scale, the *same* curve can be viewed as that for the pure Yukawa potential (ϵ independent of T).

MSA-ITEF formalism, two RHNC coexistence points are also shown. The most important observation from this figure is the strong asymmetry of the coexistence curve. This is better evidenced in reduced variables [Fig. 3(b)] by the curvature of the diameter, even close to the critical point. It should be mentioned here that the packing fraction was taken as equal to the actual volume fraction of the micelles. A different conversion of the latter into packing fractions determined form a molecular model modifies the value of the coefficients in Eq. (20) but do not suppress the ρ dependence that generates the asymmetry. The extreme case $b_0=0$ (circles in Fig. 3) indeed shows that the experimental points are not accurately reproduced when the strength is independent of ρ (the structural data are then not at all reproduced—see Fig. 3 in Ref. [19]). This means that this dependence is necessary, even though the actual values of the parameters in Eq. (20) or that of λ might be affected by a different definition of η. This impact of the dependence with ρ (compare with the case $b_0=0$) is here much more pronounced than that predicted by the vdW equation. Note that the variable on the y axis in Fig. 3 is T/T_c. In view of the previous discussion, we show in Fig. 4 the same curves together with that with $\lambda=0.73$ and ϵ independent of T (recall that this is identical to the curve with $\epsilon^*(T)=a_0+a_1T+a_2T^2$ plotted versus ϵ_c^*/ϵ^*). Whereas the temperature was found to restore symmetry within the vdW equation, we observe here that the curve with $b_0=0$ seems also strongly asymmetrical. This is clearly a consequence of a particular choice of variables. If celcius temperatures were used instead, as in some experimental studies, the diameter would not show such an ''anomalous'' slope. The inverse reduced interaction strength ϵ_c^*/ϵ^* for $b_0\neq 0$ is shown against η/η_c separately in Fig. 5.

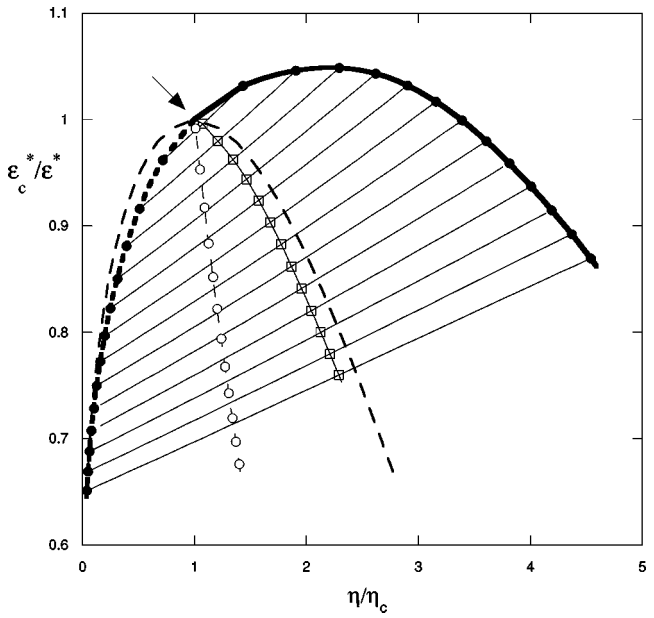

FIG. 5. Inverse reduced interaction strength for reverse micelles along the coexistence curve. Dashed lines and circles: same as in Fig. 4, ρ-independent $\epsilon(b_0=0,\lambda=0.73)$. The curve can also be viewed as the coexistence curve (the tielines, not shown, are parallel to the x axis). ρ-dependent ϵ: short dashes with dots represent vapor branch, full curve with dots represents liquid branch. The critical point is indicated by the arrow. The squares show ϵ_c^*/ϵ^* along the diameter. The tielines connecting the coexistence points at fixed T are given by Eq. (20).

This curve shows that the effective interaction strength along the coexistence curve $\epsilon^*(\rho)$ has a more ''symmetrical'' variation than the corresponding temperature $T^*(\rho)$ (the maximum value of ϵ_c^*/ϵ^* above $y=1$ at about $2\rho_c$ does not correspond to the critical point). This purely geometrical ''symmetry'' is distinct from that usually considered [25] in the theory of the liquid vapor transition. It is also different from that arising from an appropriate choice of the order parameter on the x axis (see, for example, Ref. [36] for a study of the coexistence curve of binary mixtures).

To conclude this section, it is useful to stress that a reliable assessment of the influence of the state dependence of the interaction on the coexistence curve requires a sufficiently accurate equation of state. The comparison made above of the vdW and MSA results clearly illustrated this. As a further piece of evidence of possible artifacts of approximate equations of state, we may take the example of Baxter's sticky potential [37] treated in the Percus-Yevick (PY) approximation. The latter is known to exhibit a strong inconsistency between the various routes to the thermodynamic properties, especially the virial-compressibility inconsistency. In contrast with the virial route that does not predict phase transition, the compressibility route predicts coexistence, with a strong asymmetry between the vapor and the liquid branch [38] [the crosses in Fig. 2(b) correspond to *the diameter*]. This feature has been invoked by Chen *et al.* [8] to explain the asymmetry of the coexistence curve of AOT reverse micelles. On the other hand, Barboy and Tenne [39] have shown that the same model, still treated in the PY approximation leads to a much more standard behavior of the diameter when the energy or the zero separation theorem routes are used to obtain the coexistence curve. The MSA is also not thermodynamically self-consistent, especially for strong and short-range attractions [40]) (large values of λ and ϵ). In the present case, $\lambda=1.2$ and the maximum value of ϵ is lower than k_BT. The good agreement with the RHNC and with simulations when $\lambda=1.8$ suggests that this inconsistency is not, in our case, a severe limitation. In other situations, this density-related asymmetry could be investigated by using other integral equations, preferably thermodynamically self-consistent (see, for instance, the comparison of the performances of various integral equations for the hard-core Yukawa fluid with λ1.8 in Ref. [41]).

IV. CONCLUDING REMARKS

This paper is concerned with the asymmetry of the liquid-vapor coexistence curve for a fluid with an effective interaction strength that depends on the temperature and the density. With a pure temperature dependence $\epsilon(T)$, the representations of the coexistence curve in the temperature-density and interaction strength-density planes are equivalent. The latter, however, shows that the strong asymmetry that can arise from specific forms of the law $\epsilon(T)$ in the temperature-density plane is not an intrinsic property of the coexistence curve. With a pure density dependence, the qualitative trends predicted from the van der Waals theory are correct but the magnitude of the main effects—change of the critical density and slope of the diameter—are underestimated in comparison with the results of an accurate integral equation theory. When ϵ depends simultaneously on T and ρ, the asymmetry of the coexistence curve in the T-ρ plane due to the density dependence reveals through the curvature of the diameter, even close to the critical point. The necessity to use a sufficiently accurate equation of state has also been underlined. A moderate decrease of the interactions strength was indeed detectable in the MSA treatment but not in the van der Waals one. Whether the ensuing asymmetry of the coexistence curve could be used as a signature of the density dependence of the effective potential requires clarification of the role of other sources of asymmetry. Indeed, in this work, only the interaction strength was allowed to depend on temperature and/or density. Similar investigation of the influence of the other characteristics of the interaction potential should be made before assigning with confidence the asymmetry of the experimental curves to a precise dependence of the effective interaction on the thermodynamic variables.

APPENDIX

1. van der Waals critical values with $\epsilon(\rho,T)$

When $\epsilon_1\neq 0$, there are two independent energy parameters $a_0(T)/k_BT$ and $a_1(T)/k_BT$ so the standard results for ρ_c and T_c must be reconsidered. Since the equations determining the critical point cannot be solved explicitly for arbitrary values of the parameters in Eq. (6), we resort to the small x expansion. We thus require the density dependent term $\epsilon_1\rho$ to be smaller than the constant one $\epsilon_o+\gamma T$. Since

the critical density with $\epsilon_1=0$ is insensitive to the temperature dependence, the smallness criterion becomes $x=a_1(T)b^{-1}/a_0(T)\ll 1$ or $\epsilon_1/(\epsilon_o+\gamma T_c)b\ll 1$ (this will hold also for $T>T_c$, for $\gamma>0$). One easily verifies that the expansion of ρ_c can be obtained from the result given in the text by simply replacing x by its new expression

$$\rho_c=\frac{1}{3b}\left(1+\frac{2}{3}\frac{\epsilon_1}{(\epsilon_o+\gamma T_c)b}\right).$$

This is fed into the equation

$$\left.\frac{\partial P}{\partial \rho}\right|_{T_c}=0$$

that reads $k_BT_c=(1-b\rho_c)^2[2a_0(T_c)\rho_c-3a_1(T_c)\rho_c^2]$, to obtain the new T_c as a function of ρ_c. To lowest order, the two equations can be solved explicitly [Eqs. (10)–(11) in the main text].

2. Slope of the van der Waals diameter with $\epsilon(\rho,T)$

We examine here the influence of nonlinear terms in T in the expansions of P and μ that give Eq. (4) for a_2 (the dependence on ρ does not affect the order of the expansion). At lowest order, an additional term $\frac{1}{2}p_{12}(a_1-b_1)\tau^{m+2}$ contributes to the equality of the pressures (with a similar contribution in the equation for μ). Since terms with lower exponents of τ (those involving the first derivative p_{i1} with respect to T) were already included in the expansion of Eq. (2), the results [20] $m=\frac{1}{2}$, $a_1=-b_1$, $a_2=b_2$ are unchanged. The sole modification is thus an extra term $a_1(p_{12}-\mu_{12})\tau^{5/2}$ in the final equation determining a_2. From the expansion of the free energy and using the relations $P=\rho^2(\partial(F/N)/\partial\rho)$ and $\mu=F/N+P/\rho$, one finds $p_{12}=2F_{12}+F_{22}=\mu_{12}$. Therefore, Eq. (4), giving a_2 in terms of the coefficients p_{ij}, keeps the same form.

3. Clapeyron's equation

Clapeyron's equation

$$\left(\frac{\partial P}{\partial T}\right)_\sigma=\frac{\Delta h}{T(v_g-v_l)} \tag{A1}$$

relates $\partial P/\partial T$ along the coexistence curve to the latent heat of evaporation Δh [in Eq. (A1) $v_g=1/\rho_g$, $v_l=1/\rho_l$]. Performing the differentiation with the help of the equilibrium equation (13) one gets

$$\left(\frac{\partial P}{\partial T}\right)_\sigma\left(\frac{1}{\rho_g}-\frac{1}{\rho_l}\right)=\int_{\rho_g}^{\rho_l}\frac{d\rho}{\rho^2}\left(\frac{\partial P}{\partial T}\right)_\rho. \tag{A2}$$

Inserting $(\partial P/\partial T)_\rho=(1/T)(P+a\rho^2)$ in the right-hand side of Eq. (A2) and using Eq. (13), one gets $(1/T)[P\{(1/\rho_g)-(1/\rho_l)\}+a(\rho_l-\rho_g)]$. Equations (A1) then give

$$\frac{\Delta h}{(\rho_l-\rho_g)}\rho_l\rho_g=P+a\rho_l\rho_g. \tag{A3}$$

Well below T_c, one may neglect ρ_g in the denominator of the left-hand side (lhs) of Eq. (A3), and approximate the pressure by that of the perfect gas: $P\simeq\rho_gk_BT$, giving $\Delta h\simeq k_BT+a\rho_l$. Using the relation $(\partial\Delta h/\partial T)_\sigma=\Delta c_p$ valid at $T\ll T_c$ one gets

$$\frac{d\rho_l}{dT}=\frac{1}{a}(\Delta c_p-k_B). \tag{A4}$$

The change in heat capacity at constant P, $\Delta c_p=c_{p,g}-c_{p,l}$ is easily obtained from the relations $C_p-C_v=-T(\partial P/\partial T)_V^2/(\partial P/\partial V)_T$ and $c_v^{vdW}=\frac{3}{2}k_B$. $c_{p,g}=c_{v,g}+k_B$ and $c_{p,l}=c_{v,l}+k_B/[1-(2a/k_BT)\rho_l(1-\rho_lb)^2]$ thus give

$$\frac{d\rho_l}{dT}\simeq-(k_B/a)\left[1-\frac{2a}{k_BT}\rho_l(1-\rho_lb)^2\right]^{-1}. \tag{A5}$$

The equality of the pressures at equilibrium $P_g\simeq\rho_gk_BT=P_l$ shows also that $1\gg\rho_g/\rho_l\simeq 1/(1-\rho_lb)-(a/k_BT)\rho_l$, which leads to Eq. (19) for $d\rho_l/dT$. In its turn $d\rho_g/dT\simeq(a/kT^2)\rho_l\rho_g$ follows by putting $P\simeq\rho_gk_BT$ in the lhs of Eq. (A2).

[1] T.L. Hill, *Statistical Mechanics* (Dover Publications, New York, 1987).

[2] R.J. Hunter, *Foundations of Colloid Science* (Oxford University Press, New York, 1987).

[3] C.G. de Kruif, P.W. Rouw, W.J. Briels, M.H.G. Duits, A. Vrij, and R.P. May, Langmuir **5**, 422 (1988).

[4] M.H.G. Duits, R.P. May, A. Vrij, and C.G. de Kruif, Langmuir **7**, 62 (1991).

[5] M.C. Grant and W.B. Russel, Phys. Rev. E **47**, 2606 (1993).

[6] C. Robertus, W.H. Philipse, J.G.H. Joosten, and Y.K. Levine, J. Chem. Phys. **90**, 4482 (1989).

[7] C. Cametti, P. Codastefano, P. Tartaglia, J. Rouch, and S.H. Chen, Phys. Rev. Lett. **64**, 1461 (1990).

[8] S.H. Chen, J. Rouch, F. Sciortino, and P. Tartaglia, J. Phys.: Condens. Matter **6**, 10 855 (1994).

[9] G. Cassin, J.P. Badiali, and M.P. Pileni, J. Phys. Chem. **99**, 12 941 (1995).

[10] Z. Saïdi, J.L. Darydon, and C. Boned, J. Phys. D **28**, 2108 (1995).

[11] P. Damay and F. Leclercq, J. Phys. IV **C5**, 83 (1991).

[12] M.W. Pestak, R.E. Goldstein, M.H.W. Chan, J.R. de Bruyn, D.A. Balzarini, and N.W. Ashcroft, Phys. Rev. B **36**, 599 (1987).

[13] L. Reatto and M. Tau, Europhys. Lett. **3**, 527 (1987).

[14] R.E. Goldstein and A. Parola, J. Chem. Phys. **88**, 7059 (1988).
[15] C. Domb, *The Critical Point* (Taylor & Francis, London, 1996).
[16] M. Silbert, E. Canessa, M.J. Grimson, and O.H. Scalise, J. Phys.: Condens. Matter **11**, 10 119 (1999).
[17] J.P. Hansen and I.R. MacDonald, *Theory of Simple Liquids* (Academic Press, London, 1976).
[18] C. Caccamo, Phys. Rep. **274**, 1 (1996).
[19] M. Bouaskarne, S. Amokrane, and C. Regnaut, J. Chem. Phys. **111**, 2151 (1999).
[20] J.M.H. Levelt Sengers, Ind. Eng. Chem. Fundam. **9**, 470 (1970).
[21] J.S. Rowlinson, *Liquids and Liquid Mixtures* (Butterworth, London, 1969).
[22] D. Duh and L. Mier-Y-Teran, Mol. Phys. **90**, 373 (1997).
[23] Y. Rosenfeld and N.W. Ashcroft, Phys. Rev. A **20**, 1208 (1979).
[24] F. Lado, S.M. Foiles, and N.W. Ashcroft, Phys. Rev. A **28**, 2374 (1983).
[25] B. Widom and J.S. Rowlinson, J. Chem. Phys. **52**, 1670 (1970).
[26] D.M. Heyes and P.J. Aston, J. Chem. Phys. **97**, 5738 (1992).
[27] E. Lomba and N.G. Almarza, J. Chem. Phys. **100**, 8367 (1994).
[28] A. Malijevski and S. Labik, Mol. Phys. **60**, 663 (1987); S. Labik and A. Malijevski, *ibid.* **67**, 431 (1989).
[29] S. Labik, A. Malijevski, and P. Vonka, Mol. Phys. **56**, 709 (1985).
[30] J. Clement-Cottuz, S. Amokrane, and C. Regnaut, Phys. Rev. E **61**, 1692 (2000).
[31] P. Germain and S. Amokrane, Phys. Rev. E. **65**, 031109 (2002).
[32] D. Henderson, L. Blum, and J.P. Noworyta, J. Chem. Phys. **102**, 4973 (1995).
[33] E. Waisman, Mol. Phys. **25**, 45 (1973).
[34] E.A. Guggenheim, J. Chem. Phys. **13**, 253 (1945).
[35] S.H. Chen, T.L. Lin, and M. Kotlarchyk, in *Surfactants in Solution, Vol. 2* edited by P. Bothorel and K. Mittal (Plenum, New York, 1987); S.H. Chen, T.L. Lin, and J.S. Huang, in *Physics of Supramolecular Fluids*, edited by S. Safran and N.A. Clark (Wiley, New York, 1989).
[36] P. Damay and F. Leclercq, J. Chem. Phys. **95**, 590 (1991).
[37] R.J. Baxter, J. Chem. Phys. **49**, 2770 (1968).
[38] B. Barboy, J. Chem. Phys. **61**, 3194 (1974).
[39] B. Barboy and R. Tenne, Chem. Phys. **38**, 369 (1979).
[40] M. Tau and L. Reatto, J. Chem. Phys. **83**, 1921 (1985).
[41] C. Caccamo, G. Pellicane, D. Costa, D. Pini, and G. Stell, Phys. Rev. E **60**, 5533 (1999).